Crystal Structure of the 28 kDa Glutathione *S*-Transferase from *Schistosoma haematobium*†

Kenneth A. Johnson,‡ Francesco Angelucci,‡ Andrea Bellelli,‡ Maxime Hervé,§ Josette Fontaine,§ Demetrious Tsernoglou,‡ André Capron,§ François Trottein,§ and Maurizio Brunori*,‡

Department of Biochemical Sciences and Istituto Pasteur-Fondazione Cenci Bolognetti, University of Rome "La Sapienza", Rome, Italy, and Institut National de la Santé et de la Recherche Médicale, Unité 547, Institut Pasteur de Lille, Lille, France

Received March 19, 2003; Revised Manuscript Received June 24, 2003

ABSTRACT: Schistomiasis is a debilitating parasitic disease which affects 200 million people, causing life-threatening complications in 10% of the patients. This paper reports the crystal structure of the *Schistosoma haematobium* 28 kDa glutathione *S*-transferase, a multifunctional enzyme involved in host−parasite interactions and presently considered as a promising vaccine candidate against schistosomiasis. The structures of the GSH-free enzyme, as well as the partially (∼40%) and almost fully (∼80%) GSH-saturated enzyme, exhibit a unique feature, absent in previous GST structures, concerning the crucial and invariant Tyr10 side chain which occupies two alternative positions. The canonical conformer, which allows an H-bond to be formed between the side chain hydroxyl group and the activated thiolate of GSH, is somewhat less than 50% occupied. The new conformer, with the phenoxyl ring on the opposite side of the mobile loop connecting strand 1 and helix 1, is stabilized by a polar interaction with the guanidinium group of the conserved Arg21 side chain. The presence of two conformers of Tyr10 may provide a clue about clarifying the multiple catalytic functions of Sh28GST and might prove to be relevant for the design of specific antischistosomal drugs. The K_d for GSH binding was determined by equilibrium fluorescence titrations to be ∼3 μM and by stopped-flow rapid mixing experiments to be ∼9 μM. The relatively tight binding of GSH by Sh28GST explains the residually bound GSH in the crystal and supports a possible role of GSH as a tightly bound cofactor involved in the catalytic mechanism for prostaglandin D_2 synthase activity.

Schistosomiasis is the second most devastating parasitic disease after malaria with 200 million cases worldwide, causing severe pathology in ∼10% of the patients and leading to 500 000 attributed deaths annually (*1*). Attempts to apply to schistosomiasis the technological advancements trumpeted in the genomics and structural genomics assault on diseases are limited, although initial steps have been reported on sequencing the schistosome genome (*2*). In this panorama, we report the crystal structure of the 28 kDa glutathione (GSH)[1] *S*-transferase from *Schistosoma haematobium* (Sh28GST), a promising vaccine candidate against schistosomiasis now in clinical trials (*3*).

Schistosoma mansoni 28GST (Sm28GST) was first discovered as a major antigen of schistosomiasis in the mid 1980s (*4*), and identified as a GST by sequence homology and functional assays (*5*). Mammalian GSTs have several physiological activities, including detoxification of endogenously produced compounds by means of the S-linked addition of GSH (γ-glutaminylcysteinylglycine) to electrophilic compounds to facilitate extrusion from cells, simple binding of target compounds for transport or sequestering, isomerization of steroid intermediates and other compounds, and eicosanoid biosynthesis (*6*). Soon after discovery, the schistosomal 28 kDa GSTs were investigated as potential vaccine candidates against schistosomiasis (*7*). The *S. haematobium* protein, which was shown to be the most cross-protective among the schistosomal 28 kDa GSTs, led to successful phase I and II clinical trials (*3*, *8*−*10*).

On the basis of sequence comparison, schistosomal 28 kDa GSTs would belong to the so-called sigma class of GSTs. This enzyme was shown to have high transferase activity with model compound 1-chloro-2,4-dinitrobenzene (CDNB) and also exhibited fatty acid hydroperoxide−GSH peroxidase activity (*5*). Importantly, in infected or immunized animals as well as in naturally infected humans, specific antibodies inhibit the transferase activity of schistosomal 28GSTs (*11*, *12*). Moreover, it has been reported that testosterone binds to and inhibits the transferase activity of Sh28GST (*13*). Finally, it was recently demonstrated that schistosomal 28 kDa GSTs possess prostaglandin (PG)D_2 synthase (PGDS) activity (M. Hervé, unpublished experiments), and through this property may modulate the host immune response to infection by inhibiting the migration of epidermal Langerhans cells to the draining lymph nodes (*14*). Thus, Sh28GST is a

† We are grateful to ELETTRA for a generous fellowship (to K.A.J.). This work was partially supported by the Center of Excellence in Molecular Biology and Medicine of the MIUR (Ministero dell'Istruzione, dell'Università e della Ricerca, Italy, and Agenzia Spaziale Italiana).

* To whom correspondence should be addressed: Department of Biochemical Sciences, University of Rome "La Sapienza", P.le A. Moro 5, 00185 Rome, Italy. Telephone: +39064450291. Fax: +39064440062. E-mail: maurizio.brunori@uniroma1.it.

‡ University of Rome "La Sapienza".

§ Institut National de la Santé et de la Recherche Médicale.

[1] Abbreviations: GSH, reduced glutathione; GST, GSH *S*-transferase; Sh28GST, 28 kDa GST from *S. haematobium*; PGDS, prostaglandin D_2 synthase; H-PGDS, hematopoietic PGDS; CDNB, 1-chloro-2,4-dinitrobenzene.

10.1021/bi034449r CCC: $25.00
Published on Web 08/02/2003

multifunctional enzyme which plays key roles in the host−parasite interactions. In this work, we present the high-resolution structures of Sh28GST, at different levels of saturation with GSH.

MATERIALS AND METHODS

Expression, Purification, and Preparation of Sh28GST for Crystallization. The full-length cDNA of Sh28GST was subcloned into pET-24d(+) (Novagen), and *Escherichia coli* BL21(DE3) cells were transformed with this expression vector (M. Hervé, unpublished experiments). Purification of Sh28GST was carried out as previously described (*15*). Initially, the recombinant protein was purified by affinity chromatography on a GSH-conjugated Sepharose column, and eluted at pH 7 using GSH. However, to obtain an enzyme preparation without bound GSH, the recombinant Sh28GST was affinity-purified twice on GSH-conjugated Sepharose columns using 50 mM glycine (pH 10) as the eluant (*16*). After elution, the protein was dialyzed extensively in phosphate-buffered saline (PBS, pH 7.4) containing 1 mM dithiothreitol, passed through polymyxin columns, concentrated to 66 mg/mL by ultrafiltration (Amicon PM10), and sterile-filtered.

Crystallization. Crystals were obtained under conditions similar to those reported for Sm28GST (*15*). Sh28GST was crystallized by the hanging drop vapor diffusion method using a well solution of 2.1 M ammonium sulfate, 100 mM Tris (pH 7.2), and 5 mM β-mercaptoethanol. The hanging drops consisted of a 1:1 mixture of the well solution with the solution of protein at 66 mg/mL in PBS. Large crystals grew within a few days. Crystals of the GSH-saturated enzyme were obtained from protein equilibrated with a 500 μM excess of GSH prior to crystallization trials. Crystals of the GSH-free enzyme were obtained following essentially the same procedure, starting with the enzyme prepared in the absence of GSH.

Data Collection and Processing. Data for the two structures were collected at ELETTRA (Trieste, Italy) and at DESY (Hamburg, Germany) at ~100 K. Data were processed with the HKL suite (*17*). Autoindexing produced a list containing two likely choices for the space group and unit cell with equivalent scores, either $C222_1$ or $P2_1$. The data from a home source and detector [Rigaku R-axis IV++ detector, coupled to an RU-200 rotating anode X-ray (Cu Kα) generator equipped with focusing mirrors and operating at 50 kV and 100 mA] to 2.1 Å were used to determine the structure. The data were originally processed in space group $C222_1$ with one Sh28GST monomer in the asymmetric unit and the following cell dimensions: $a = 72.6$ Å, $b = 77.4$ Å, and $c = 77.7$ Å. During refinement of the first structure, it appeared likely that the second possibility (space group $P2_1$, $a = 53.1$ Å, $b = 77.7$ Å, $c = 53.2$ Å, and $\beta = 93.4°$ which has a dimer of Sh28GST in the asymmetric unit) was after all the correct choice (see below). Thus, the two data sets used for refinement were processed using the $P2_1$ unit cell.

Molecular Replacement, Model Building, and Refinement. The structure was determined by molecular replacement in the $C222_1$ unit cell. The ninth search model which was used, the structure of Sj26GST (PDB entry 1gtb), resulted in a clear rotation and translation solution using the program AMORE (*18*) from the CCP4 suite (*19*). The structure was refined using REFMAC (*20*), and fit to electron density maps using XtalView (*21*). However, even after the addition of many observed waters, the *R*-factor converged to 26% which clearly indicated a problem with the structure. The most likely problem was with the choice of space group especially given the almost identical length of the *b* and *c* axes. Thus, the structure was transferred to the $P2_1$ unit cell and refined easily, leading to a final R_f of less than 23% for both structures. The two monomers in the $P2_1$ asymmetric unit are very similar (see the text) but do exhibit fine differences especially in the active site. This special case of twinning arises from the combination of very similar monomers and the almost identical length of the *b* and *c* axes. Thus, the noncrystallographic 2-fold axis of the dimer found in the $P2_1$ space group can be "twinned" to a crystallographic 2-fold axis in space group $C222_1$.

Equilibrium Fluorescence Titrations. The affinity of Sh28GST for reduced GSH was determined by taking advantage of the tryptophan fluorescence quenching occurring upon combination binding (*22*). The experiments were carried out using a Spex Fluoromax spectrofluorimeter in 0.1 M potassium phosphate (pH 7). Sample solutions of Sh28GST were prepared by diluting the stock to concentrations ranging between 0.1 and 5 μM and adding reduced GSH (Sigma, St. Louis, MO); usually the dilution due to addition of the titrant was negligible. The excitation wavelength was 280 nm, and emission spectra were collected over the range of 300−400 nm; emission peaked at 337 nm, and readings at this wavelength were used for the quantitative analysis. Measurements were carried out using the two preparations of protein, one purified by elution form the GSH affinity column with glycine at pH 10 and the other with GSH at pH 7 (see above). Addition of GSH up to ~1 μM induced a 30% Trp fluorescence quenching; however, in some experiments, further quenching ($\leq$10%) was observed upon addition of very large amounts of GSH (up to 0.1 M), suggesting the possible existence of low-affinity GSH binding sites, as already reported for similar proteins (*23*).

Stopped-Flow Fluorescence Measurements. Stopped-flow experiments were carried out using an Applied Photophysics (Leatherhead, U.K.) MV18 apparatus equipped for fluorescence signal detection. The excitation wavelength was 285 nm, and emission was collected using a filter with cutoff at $\geq$320 nm. Solutions of Sh28GST (10 μM) in 0.1 M phosphate (pH 7) were mixed with buffered solutions of GSH at concentrations ranging between 15 and 80 μM. The transmittance of the samples at 285 nm was higher than 75% (with a 1 cm path length). The time courses were fitted to a pseudo-first-order equation to obtain the apparent combination rate constants k_{app}. Linear regression of k_{app} versus the concentration of GSH yielded the intrinsic rate constants for combination (k_{on}) and dissociation (k_{off}) of GSH.

Steady State Determinations. The catalytic activity of Sh28GST was measured spectroscopically under steady state conditions, using the chromogenic substrate 4-chloro-1,2-dinitrobenzene (CDNB, Sigma). Two typical assays were performed, either at a fixed GSH concentration or at a fixed CDNB concentration. In the former case, the sample was prepared as follows. A 0.33 μM solution of Sh28GST (0.5 mL) in 0.1 M potassium phosphate buffer (pH 7) was pipetted into a 2 mm spectrophotometric cuvette; then GSH was added to a final concentration of 2 mM. The reaction was started by addition of the appropriate volume of a 0.25

Table 1: Data Collection and Refinement Summary

	structure 1 (≈40% GSH-saturated)	structure 2 (≈80% GSH-saturated)
space group	$P2_1$	$P2_1$
no. of unique reflections	39246	51735
$I/\sigma(I)$	21.5 (3.4)[a]	40.9 (2.7)[b]
completeness (%)	96.3 (72.0)[a]	99.2 (95.0)[b]
average redundancy	6.5 (2.6)[a]	4.1 (2.8)[b]
final R_{merge}	0.071 (0.22)[a]	0.04 (0.47)[b]
unit cell edges (Å)	$a = 53.43$, $b = 78.11$, $c = 53.50$	$a = 53.14$, $b = 77.71$, $c = 53.20$
unique angle β (deg)	94.2	93.4
$R_{working}$ (R_{free})[c]	0.229 (0.289)	0.229 (0.280)
rms deviation		
bond lengths (Å)	0.024	0.023
bond angles (deg)	1.6	1.3
Ramachandran plot		
most preferred	335	338
allowed	24	24
generously allowed	2	1
disallowed	0	0
model composition		
no. of water molecules	226	317
no. of ligand molecules	1 (GSH)	1 (GSH)

[a] Last shell (1.86−1.81 Å) in parentheses. [b] Last shell (1.71−1.65 Å) in parentheses. [c] $R = \sum||F_o - F_c||/\sum|F_o|$, where F_o and F_c are the observed and calculated amplitudes, respectively. The free data comprised 5% of the total.

M solution of CDNB in 95% ethanol; the final volume ranged between 0.510 and 0.525 mL (*24*). The reaction was followed by the absorbance increase at 340 nm in a Hewlett-Packard diode array spectrophotometer. The alternative experiment was carried out in a similar way, at a constant concentration of 2.5 mM CDNB. To check the effect of praziquantel on the catalytic activity of Sh28GST, if any, the following method was adopted. Several stock solutions of praziquantel (Sigma) in methanol were made at 100× for each experiment, thus keeping the concentration of methanol at a constant 1%. These 100× stock solutions were used to add praziquantel to the reaction mixture, prior to the addition of the second substrate, to achieve final concentrations in the range of 0−1 mM.

RESULTS

Quality of the Structure. The two Sh28GST crystal structures initially illustrated here, i.e., that of a partially GSH-saturated protein (the first structure) and that of a protein cocrystallized with saturating GSH (the second structure), were refined using high-resolution data, 1.85 and 1.65 Å, respectively, with each model achieving final *R*-factors of 22.7 and 22.8%, respectively (Table 1). The distribution of main chain angles in both models shows 93.7% falling in the preferred region of a Ramachandran plot with the remaining 6.3% in the allowed region, and none in the less favorable generously allowed region. Only Glu70, found in the tight turn between β-strand 4 and helix 3 (see below), exhibits unusual main chain angles, which however were found in all other GSTs for the Gln, Glu, or Asp at this position. These unusual main chain angles are thought to arise from the dual function of this residue which is involved in contributing to the dimer interface but also forms part of the binding site for GSH (*25*). The geometry of both models is good, given that the geometric restraints which were used during refinement of the models led to root-mean-square deviations that were canonical for average bond distances and angles of structures at these resolutions. Analysis of the many geometrical factors of the two final models gives an overall resulting "goodness" or *g*-factor which is also at the mean for structures at similar resolution (*26*). The two structures have been deposited in the Protein Data Bank as entries 1OE7 and 1OE8.

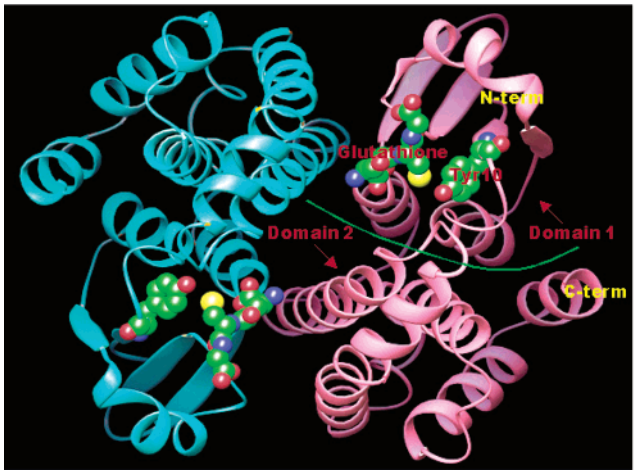

FIGURE 1: Ribbon-style view of the GSH-saturated Sh28GST dimer, showing the bound GSH and the activating conformer of active site residue Tyr10. Each monomer is composed of two domains. The N-terminal domain (denoted as domain 1) has a thioredoxin-like fold consisting of a four-stranded β-sheet (order 2134) surrounded by three α-helices, and the C-terminal domain (denoted as domain 2) is composed entirely of α-helices. The N-terminal domain serves mainly to bind GSH, whereas the C-terminal domain forms the xenobiotic binding site. The two monomers are indeed very similar; fine differences in the active sites are discussed in the text.

Overall Structure. Sh28GST is a dimer, each monomer having the typical N- and C-terminal domains (Figure 1) making up the canonical GST fold. The model contains residues 4−207 in each monomer. The N-terminal domain (residues 4−87), which consists of a four-stranded β-sheet (order 2134) flanked by three helices, forms a thioredoxin-like fold. The C-terminal domain (residues 88−207) consists of six α-helices, or seven if helix 5a and helix 5b are considered separate helices. The N-terminal domain forms

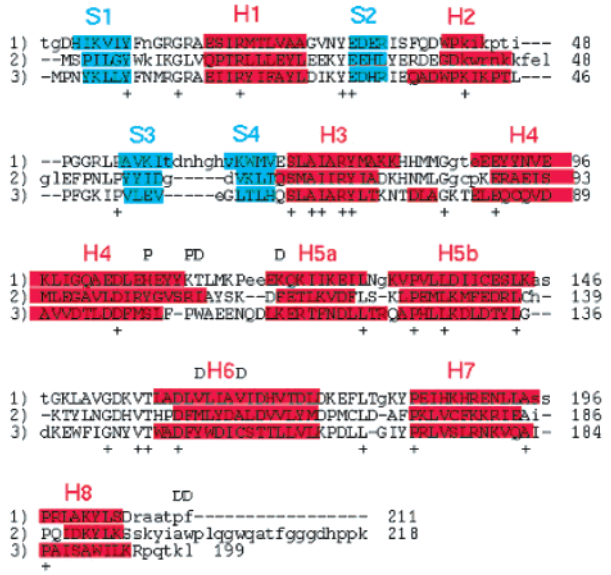

FIGURE 2: Structure-based sequence alignment using the program SEQUOIA of (1) Sh28GST and two structures discussed in the text, i.e., (2) *S. japonicum* 26 kDa GST with bound praziquantel [Sj26GST, PDB entry 1gtb, 2.2 Å root-mean-square deviation (rmsd) for superposition of 176 equivalences with 46 identities] and (3) the hematopoietic prostaglandin D synthase (HPDS, PDB entry 1PD2, 1.7 Å rmsd for superposition of 192 equivalences with 61 identities). Equivalent residues (capital letters) are those which after superposition are within 3 Å of the corresponding residues in Sh28GST. Helices are denoted in red and strands in cyan. Y104 and R108, the two residues that in Sj26GST interact with bound praziquantel, are marked with a P. A D appears above residues in HPDS which contribute to the putative prostaglandin binding cleft. Residues Tyr10, Arg16, and Arg21 are discussed in the text.

the binding site for GSH, called the G-site, whereas the C-terminal domain provides the residues of the H-site where the electrophilic substrate is bound. The two monomers, called A and B, are very similar but not identical, at least in the structure collected at high GSH concentrations; on the other hand, they are indistinguishable in the structure of the GSH-free enzyme.

The typical overall fold is maintained despite the quite low degree of sequence similarity with other GSTs. This is illustrated by a structure-based sequence alignment of Sh28GST with (i) the *Schistosoma japonicum* 26 kDa GST [Sj26GST, PDB entry 1GTB (*27*)] which was used to determine the structure by molecular replacement and (ii) the structure in the Protein Data Bank whose sequence is most identical to that of Sh28GST (32%), i.e., that of rat hematopoietic PGDS [H-PGDS, PDB entry 1PD2 (*28*)] (see Figure 2). Sh28GST, like H-PGDS and the sigma class GSTs, lacks a long C-terminal extension which occludes the active site in Sj28GST and alpha class GSTs. One distinguishing feature of the Sh28GST fold as compared to other GSTs is the increased length of the β-sheet, which is also evident as a gap in the sequence alignment between strand 3 and strand 4 (Figure 2).

The crystallographic structure of Sh28GST is compatible with the expectation that the protein forms a dimer in solution, as do most GSTs (*29*, *30*). The dimer interaction surface area in the crystal (1142 Å^2 and 137 short contacts of $\leq$4 Å) is dominated by nonpolar interactions but has 21 polar interactions, including four salt links. The relatively high ratio of polar to total contacts (21/137) identifies Sh28GST as having a dimer interface similar to those of the sigma class GSTs (*6*, *31*). The overall buried surface area, however, is at the low end of the range typical for GSTs, with monomer−monomer surface areas ranging from ~1000 to ~2000 Å^2 (from the Protein Quaternary Structure Server at EMBL-EBI). Like the sigma class GSTs, Sh28GST lacks the hydrophobic "lock-and-key" motif found in the dimer interface of the alpha, pi, and mu classes of GSTs (*6*). The level of sequence identity of Sh28GST with nonschistosomal GSTs is at most 32%, which would tend to place the schistosomal GSTs in a separate class given that the cutoff of ~30% sequence identity has been suggested to distinguish GST classes (*6*). Schistosomal 28 kDa GSTs are highly homologous, with the lowest level of pairwise sequence identity being 77% (*32*).

GSH Binding Site. Our initial structure proved to be partially saturated with GSH despite extensive dialysis against phosphate-buffered saline prior to crystallization; the active site in each monomer appears to be somewhat less than 50% saturated with GSH in the crystal. The occupancy of GSH was estimated by comparing the *B*-factors of the C_α atoms from GSH with those of the polypeptide chain that interact with it (e.g., Glu70). A second structure was obtained by crystallizing Sh28GST exposed to 3.3 mM GSH prior to crystallization; this structure was little changed except that the fractional saturation with GSH was higher (Figure 3, top panels). Preliminary crystallographic data obtained at a still higher GSH concentration (15 mM) suggest an even higher occupancy. These data are consistent with the hypothesis that the binding of GSH to Sh28GST may display negative cooperativity, a point to be further investigated.

Sh28GST is characterized by a unique feature which, to the best of our knowledge, has not been reported for other GSTs, since the crucial and invariant active site Tyr10 side chain occupies two distinct positions in each monomer (Figure 3). Tyr10 has been proposed (*29*, *30*) to interact with and help form the active thiolate of GSH by lowering the pK_a of the sulfhydryl group from 9 to 6−7. There is no obvious relationship between the percentage of bound GSH and the dual position of the Tyr10 side chain, the two conformers being almost equally populated (as judged from the *B*-factors) in all the structures of Sh28GST. The description of the Sh28GST structure discussed below refers to the one collected in 3.3 mM GSH (approximately 80% GSH saturated) except where stated differently. Preliminary crystallographic data obtained at a still higher GSH concentration (15 mM) seem to indicate that the relative amount of the two alternative conformers of Tyr10 may be altered, even though no experimental condition was found to induce Tyr10 to adopt completely the activating position.

GSH is bound to both monomers in the extended conformation, as observed in all other GST−GSH complexes (*33*), and forms salt links with three residues from the N-terminal domain (Arg16, Lys45, and Glu70) of the same monomer and a fourth one with Asp104 from the C-terminal domain of the other monomer. Since the side chain of Arg16 is also found in two conformations, the number of salt links might be counted as fewer than four. In addition, GSH forms three H-bonds with protein main chain atoms and seven H-bonds with protein side chain atoms, all from the N-terminal domain of the same monomer. There are also four H-bonds to water molecules, including one to the sulfur thiolate of GSH in

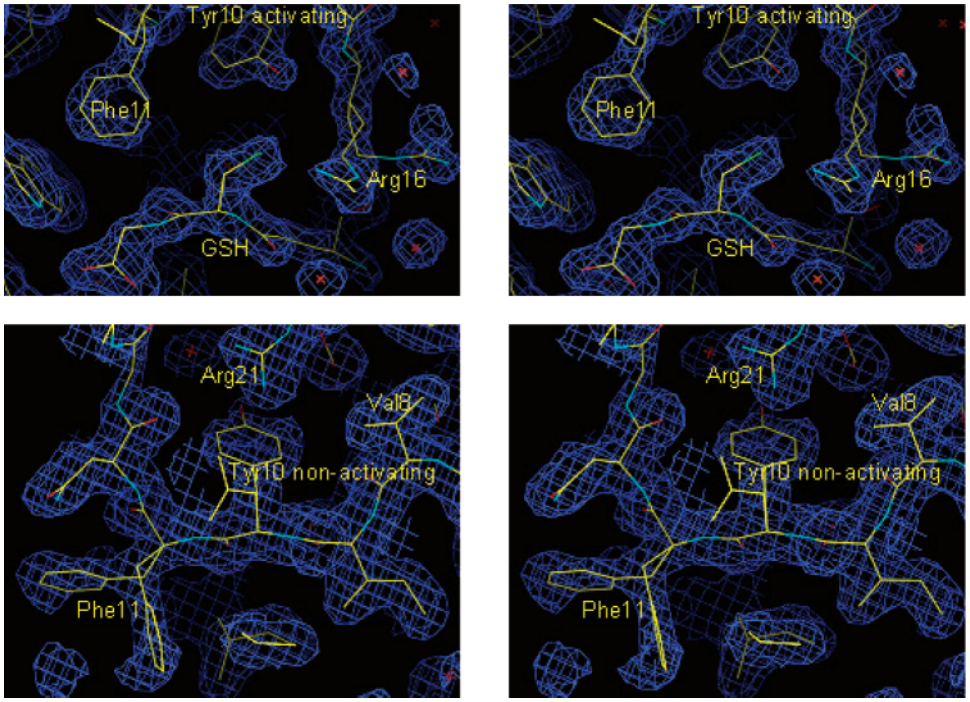

FIGURE 3: Stereoview of the electron density ($2F_o - F_c$ at 1σ; blue contours) showing evidence for two conformers of Tyr10 in the active site of monomer B, from the structure which is almost fully saturated with GSH. The stick model uses yellow for carbon, red for oxygen, blue for nitrogen, and green for sulfur. The top panels illustrate the level of disorder in three active site residues, namely, Phe11, Tyr10, and Arg16. The side chain of Tyr10, shown in the activating conformation, forms H-bonds with the S atom of GSH and the main chain N atom of Arg16. The guanidinium group of Arg16 forms an H-bond with the S atom of GSH and a salt link with the carboxylate group of the γ-Gln of GSH. For Phe11, only one conformer is shown. The bottom panels show the nonactivating conformer of Tyr10 (center) and its polar interaction with the side chain of Arg21 (at the top). The activating conformer of Tyr10 is only partly visible (facing into the page). The two conformers of Phe11 are clearly seen.

the A monomer; it is likely that this water plays a role in stabilizing the ionized state of bound GSH. In comparison, a survey of GSH−protein contacts in high-resolution structures in the Protein Data Bank [alpha class 1F3A (*34*), pi class 8GSS (*35*), mu class 6GST (*36*), and Sj26GST 1GNE (*37*)] reveals three salt links for the alpha, pi, and mu class GSTs and two for the Sj26GST. In addition, the mu class GSTs form two H-bonds with protein main chain atoms, whereas the alpha class, pi class, and Sj26GST proteins form three H-bonds with protein main chain atoms.

As stated above, two side chains in the G-site have dual conformations, those of the aforementioned Tyr10 and Arg16 (Figure 3, top and bottom panels). In the canonical position, the hydroxyl oxygen of Tyr10 makes an H-bond with the sulfur atom of GSH which stabilizes the activated, nucleophilic thiolate. In all other GST structures with an active site tyrosine, that is for the alpha, pi, mu, and sigma classes (*29*, *30*), this activating conformer is the only one observed. In contrast, in the GSH-free enzyme as well as the two GSH-bound structures (partially and almost fully saturated), the Tyr10 side chain is found in the canonical activating conformer at approximately 50% occupancy. Both conformers of Tyr10 are stabilized by polar interactions. The activating conformer is stabilized by (i) an H-bond between the hydroxyl oxygen of Tyr10 and the main chain N atom of Arg16 (as observed in all the other structures of GST−GSH complexes) and (ii) an H-bond with the sulfur atom of GSH *but* only in the B monomer. The nonactivating conformer of Tyr10 is stabilized by an electrostatic interaction with the guanidinium group of the side chain of Arg21 in both monomers.

The side chain of Arg16 also displays a dual conformation, with one conformer forming a salt link with the carboxylate moiety of the γ-glutamine of bound GSH and the other forming an H-bond with the sulfur atom of GSH, as in alpha class GSTs (*30*). Inspection of the maps (Figure 3, top panels) reveals more electron density surrounding the activating conformer in the GSH-saturated enzyme. Thus, the conformer of Arg16 which interacts with the GSH sulfur atom appears to have a higher occupancy when the active site is almost fully GSH saturated.

A third residue in the active site, i.e., Phe11, appears to have more than one conformation (Figure 3, bottom panels). The major conformer, observed most clearly in the highest-resolution structure of the GSH-saturated complex, places the side chain in an unstable position which contacts the side chain of Phe38 in a symmetry-related molecule belonging to another dimer in the crystal unit cell. It is likely that the side chains of Phe11 and Phe38 lie in multiple conformers which make stable crystal contacts but which differ throughout the crystal. The major conformer, similar to that observed in other structures of GSTs, is one which has been demonstrated to play a second-tier role in activating the sulfur atom of GSH by acting to lower the pK_a of the Tyr10 hydroxyl group (*38*).

Comparison of the G-Site in A and B Monomers. Asymmetry between the A and B monomers in the homodimer is extremely weak, and is limited to the details in the positions of some amino acid residues in the G-site. In any case, the weak asymmetry between the two monomers does not significantly correlate with the alternative conformations of Tyr10, Arg16, and Phe11. The difference in the two

monomers is amplified by the position of GSH, since the orientation of the S atom is different in the A and B monomers. Comparison reveals some differences in geometry around the all-important sulfur atom of bound GSH. In the A monomer, the Tyr10 hydroxyl of the activating conformer is 4.5 Å from the S atom of GSH; close to this atom are also a water (within 2.95 Å) and the NH1 atom of Arg16 (2.86 Å from the S atom). In the B monomer, the Tyr10 hydroxyl in the activating conformation is at a distance of 3.4 Å and the NH1 atom of Arg16 is 2.64 Å from the S atom of GSH, with no water within H-bonding distance. The calculated distances for the H-bonds between a negatively charged S atom and a hydroxyl group, or between a negatively charged or neutral S atom and a variously charged water molecule, have been reported (refs *39* and *40*, respectively). These calculated distances suggest that in the A monomer, the sulfur atom of GSH is negatively charged, a thiolate, and makes one H-bond with a positively charged water molecule; on the other hand, the Tyr10 hydroxyl oxygen at 4.5 Å is too distant from the S atom to form an H-bond. In contrast, in the B monomer, the Tyr10 hydroxyl oxygen (3.5 Å) is likely to be neutral and protonated and to form a stable H-bond with the negatively charged S atom. In both the A and B monomers, the NH1 atom of Arg16 is probably also positively charged and within H-bonding distance, though calculations were not reported for this type of atom.

The structures of all other GSTs show that invariant Tyr10 is present only in the activating conformation, which is most relevant for catalysis. The structure of Sh28GST reveals that, at least in the crystal, Tyr10 occupies a nonactivating conformation (see above). Our data do not allow us to precisely estimate if the fraction of Tyr10 in the two alternative conformations is the same in both the A or B monomer; however, the relevant electron densities and *B*-factors are comparable in the two monomers, and thus, we conclude that the two conformers of Tyr10 are approximately equally populated in both monomers of the active Sh28GST dimer.

Comparison of PGDS and Sh28GST H-Site. GSTs in general catalyze the nonspecific conversion of the prostanoid precursor PGH_2 to three products: PGD_2, PGE_2, and PGF_2 (*41*). A class of GSTs which catalyzes the specific conversion of PGH_2 to PGD_2 has been described (*42*), and for rat H-PGDS (sequence in Figure 2), the crystal structure has been published (*28*, *43*). Sh28GST, whose sequence is 32% identical to that of rat H-PGDS, has been identified as a specific PGDS (M. Hervé, unpublished experiments). In the H-PGDS structure, there are two clefts near the G-site which have been proposed to bind the J- and K-arms of the prostanoid precursor, PGH_2. In Sh28GST, the side chains of Glu106, Tyr110, and especially His169 would interfere with binding of PGH_2 in the same mode proposed for H-PGDS. Specifically, the side chain of His169 is sterically hindered from moving and forms two H-bonds, the first between the NE2 atom and the main chain O atom of Arg14 and the second between the ND1 atom and the side chain OE1 atom of Glu106. However, the H-site near the bound GSH in Sh28GST is very open with space for both the approach of the PGH_2 headgroup near the GSH thiolate and the positioning of both arms of the substrate in contact with the protein surface.

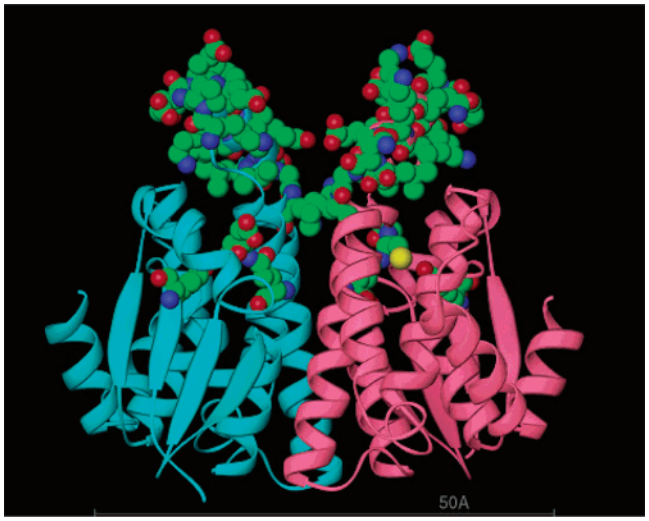

FIGURE 4: Ribbon-style view of the Sh28GST dimer showing the location of residues 115−131 (top) which make up the cross-protective antigen and its typology and distance from the active site. Also shown are the bound GSH (center) and the active site Tyr10 (center left and center right) in the activating conformer. These antigenic peptides, located near each other on the protein surface, contain many charged residues but do not contribute to the stability of the monomer−monomer interface (since they form no stabilizing contacts in the Sh28GST dimer). Carbon atoms are shown in green, oxygens in red, and nitrogens in blue, and the sulfur of GSH is shown in yellow.

Helix 5A Major Antigenic Peptide. Natural antibodies to schistosomal GSTs are known to inhibit the transferase activity (*11*); however, this effect is not due to antibodies against the most potent antigenic and cross-reactive region of the protein molecule, identified from investigations of various antigenic peptides of schistosome 28GSTs as the Pro115−Lys131 fragment. This region may be important in the cross-protection against different schistosome species, including *S. mansoni*, *S. haematobium*, and *Schistosoma bovis* (*32*). In the crystal structure, this peptide contains the last part of the loop between helix 4 and helix 5a up until the first residue of helix 5b. The Pro115−Lys131 peptides in the A and B monomers are located topologically close to each other and near the G- and H-sites, as shown in Figure 4.

Kinetic Characterization of Sh28GST. The finding that Sh28GST is partially saturated with GSH in the first crystal structure, despite extensive dialysis prior to crystallization, indicated that GSH is bound tightly. To measure the affinity of Sh28GST for GSH, we exploited the decrease in fluorescence of the protein upon GSH binding, mostly attributed to a change in the environment of Trp 41 which forms an H-bond between its side chain NE1 atom and the carbonyl oxygen of the glycine moiety of bound GSH (*22*). Titrations of Sh28GST at very low concentrations (0.1 μM) with GSH under equilibrium conditions were carried out for the two preparations of the protein; as shown in Figure 5A, we obtained similar results with a fitted K_d of $\simeq$3 μM. In addition, we employed stopped-flow fluorescence measurements to follow the time course of GSH binding which conformed in all cases to a simple exponential. The estimate of the affinity for GSH from these experiments is model-dependent and assumes second-order, reversible binding to independent monomers; this expectation is consistent with the experimental observations (Figure 5B). The stopped-flow

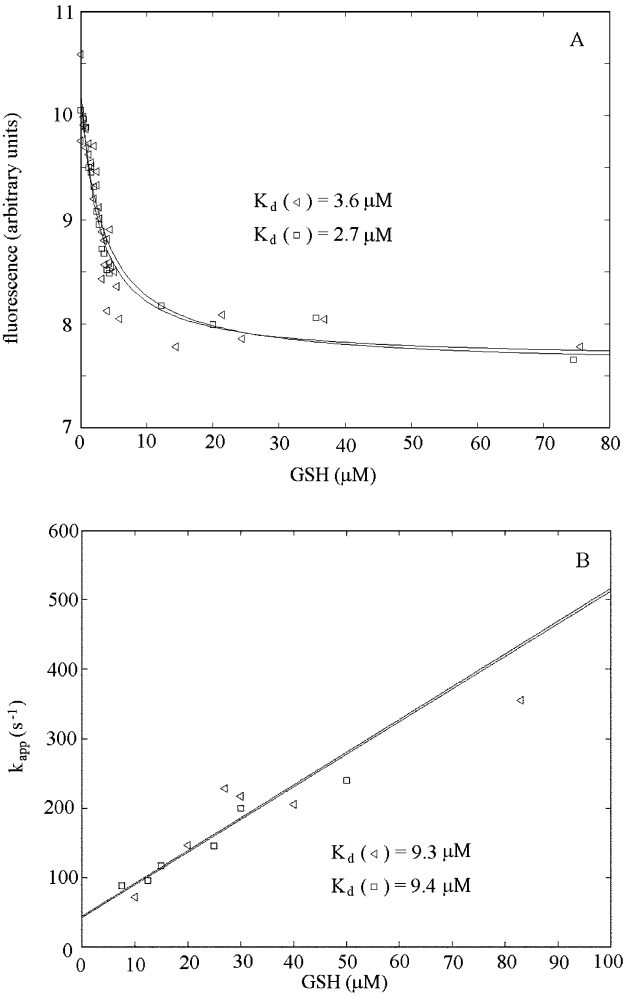

FIGURE 5: Measurements of affinity of Sh28GST for GSH by equilibrium fluorescence titration (A) and stopped-flow kinetics (B). Experiments were carried out with two enzyme preparations purified using either GSH (squares) or glycine (triangles) to elute the protein from the GSH−Sepharose affinity column. The two enzyme preparations gave similar K_d values for GSH binding, by both methods. Conditions: 0.1 M phosphate buffer at pH 7 and 20 °C with 0.2 μM Sh28GST.

experiments, also carried out on both batches of the protein, yielded an estimated K_d of 9 μM. Both estimates of K_d (3 μM by equilibrium and 9 μM by kinetics) are similar to the smallest previously reported values (e.g., 7 μM for an alpha class rat liver GST) (*23*), and are significantly lower than the usual range of ≥300 μM. Thus, Sh28GST has an affinity for GSH which ranks among the highest, up to 100 times higher than values usually reported for GSTs.

The transferase activity with CDNB, measured as detailed in Materials and Methods, corresponds to a specific activity of 12 μmol of product formed per minute per milligram of protein, similar to those found for other GSTs, including H-PGDS (*44*, *45*). The effect of praziquantel (PZQ, an antischistomial drug which was formerly thought to combine with GST) (*27*) was checked in a steady state experiment. The assay contained GST (330 nM), GSH (2 mM), and CDNB (2.5 mM) and variable concentrations of PZQ, from 0 to 1 mM. Relatively high GSH concentrations were used throughout because this probably approximates the condition occurring in the cell. All the data obtained from 0 to 1 mM PZQ showed no effect on the Sh28GST activity. Since the drug does not affect the functional properties of the enzyme (at least under our experimental conditions), it seems unlikely that its main pharmacological target is GST. Our results are consistent with those published by Milhon et al. (*46*), and indicate that the pharmacological effect of PZQ at the clinically relevant concentration of 13 μM (*27*) cannot be due to inhibition of Sh28GST.

Though PZQ was reported not to inhibit the transferase activity of Sj26GST, the structure of Sj26GST from crystals grown in the presence of PZQ did show a molecule of the drug bound at the dimer interface but distant from the active site (*27*). This PZQ binding site in Sj26GST was said to be preformed in the apo-Sj26GST structure and was in a location similar to the one described as a transport binding site in a alpha class GST (*47*). An inspection of the same location in the Sh28GST structure reveals that side chain movements of several angstroms would be required to reveal a similar binding site for PZQ. This observation, together with an inspection of the sequence alignment between Sj26GST and Sh28GST (Figure 2), suggests that PZQ does not bind to Sh28GST. Thus, we conclude from kinetic and structural data that Sh28GST is unlikely to be the target enzyme accounting for the antischistosomal activity of PZQ.

DISCUSSION

In comparison to other reported GST structures, the residues in the active site of Sh28GST exhibit dual side chain conformers (Tyr10, Phe11, and Arg16). The invariant active site Tyr10 has been extensively studied because of its essential role in the transferase mechanism (*30*). As far as we know, the nonactivating conformer of Tyr10 clearly seen in the Sh28GST structure has never been reported before for any of the several GSTs containing Tyr at this position. In Sh28GST, the two conformers of Tyr10 illustrated above have similar occupancies in all the independent structures despite the fact that one of them was obtained for a protein which had been pre-equilibrated with a saturating concentration of GSH prior to crystallization, thus allowing any possible rearrangements of structure to take place in solution.

To investigate conditions which might alter the distribution of the two conformers of Tyr10, two more structures were collected at the DESY synchrotron. The structure of the GSH-free Sh28GST at pH 7.0 was determined starting from the enzyme preparation purified using glycine instead of GSH (see Materials and Methods); in addition, starting from the enzyme that was partially GSH saturated, we collected a data set for a crystal soaked at pH 8.0 to rule out the possibility that the bound GSH sulfhydryl had a pK of >6.2−6.5, as reported for other GSTs (*30*). However, both structures (data not shown) exhibited the same occupancies for the two conformers of Tyr10. In summary, the three structures at pH 7.0 (GSH-free, partially saturated, and almost fully saturated) exhibit similar relative occupancies of the two Tyr10 conformers (Figure 6). Because the GSH-free and saturated enzymes were crystallized starting from a protein fully equilibrated in solution prior to crystallization, it is likely that the distribution of conformers found in the crystal would be present also in solution. Moreover, the pH 8.0 data demonstrate that either an unusually high pK for bound GSH or an unusually low pK of Tyr10 (*48*) is unlikely to control the relative population of the two Tyr10 conformers. Can the tyrosine swing in the crystal structure? The two conformers of Tyr10 are both stabilized by specific polar interactions

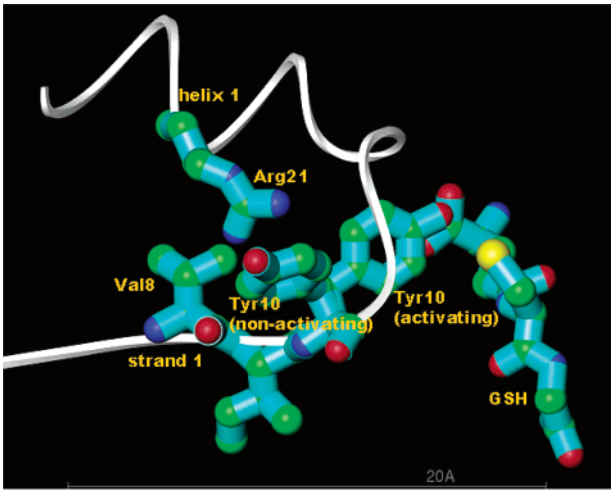

FIGURE 6: Ball-and-cylinder representation of the two Tyr10 conformers in the B monomer of the almost fully saturated enzyme, with a ribbon-style (white) representation of β-strand 1 and α-helix 1. Carbon atoms are in green, oxygens in red, and nitrogens in blue, and sulfur is shown in yellow. The activating conformer of Tyr10 forms an H-bond with the S atom of GSH; the nonactivating conformer forms a polar interaction with the guanidinium group of Arg21. Interconversion between the two conformers of Tyr10 is blocked in the crystal structure by the side chain of Val8 and the loop between β-strand 1 and α-helix 1.

(see Results) as well as favorable steric contacts. As shown in Figure 6, rotation of the Tyr10 side chain about the $C_\alpha-C_\beta$ bond is blocked in one direction by the main chain of the loop between β-strand 1 and helix 1, and in the other by the rather rigid side chain of Val8, which is on the same β-strand as Tyr10. Thus, it is very unlikely that the two conformers can interconvert in the crystal.

In solution, large conformational changes between apo and GST-bound forms of several GSTs have been described (*49*−*51*). In the human P1-1 pi class GST, a disulfide bond can be formed between two cysteines which are 18 Å apart in the crystal structure (*52*, *53*). In the same GST, the short 3_{10}-helix 2 is disordered in the apo form but ordered in the GSH-bound enzyme (*51*). In Sh28GST, the short helix 2 is both preceded (Phe-Gln-Asp) and followed by a three-residue (Lys-Pro-Thr) 3_{10}-helix which suggests a similar flexibility. In addition to conformational fluctuations in tertiary structure, a specific structural rearrangement of the G-site upon binding of GSH has been suggested for several GSTs (*49*).

The Sh28GST structure exhibits features of the barriers to the formation of the active thiolate which would lead to monomer heterogeneity, that is, the presence of both active and inactive conformers. As discussed above, the Tyr10 side chain must reside in the activating conformer to form the crucial H-bond with the sulfur atom of GSH (see Figure 6). Moreover, the water molecule H-bonded to the thiolate in monomer A of the Sh28GST structure must be displaced to free the thiolate for transferase activity. All of the above suggests that a conformational change should be involved in the activation of the thiolate.

Since Arg21 (a highly conserved residue in all classes which share a catalytic active site tyrosine) helps to stabilize the nonactivating conformer of Tyr10, we suggest that this conformer may not be unique to Sh28GST. In fact, an inspection of other GST structures (*27*, *31*, *35*) reveals that the side chain of the arginine homologous to Arg21 displays a conformation similar to that seen in Sh28GST. In other GSTs, water molecules fill the space near the guanidinium group that a nonactivating Tyr10 conformer (if present) would occupy, requiring a slight rearrangement of structure to make room for the phenoxyl group. If a nonactivating conformer were accessible to other GSTs, it might account for the "half-of-the-sites" reactivity reported for some of these enzymes; e.g., in human GST A1-1, half-of-the-site reactivity was observed to occur for additions to three different substrates, irrespective of the concentration of GSH (*16*). This finding is consistent with our observation that the relative occupancies of the activating and nonactivating Tyr10 conformers in the Sh28GST crystal structure are poorly sensitive to the degree of GSH saturation of the enzyme.

Since mammalian sigma class GSTs, as well as several GSTs from invertebrates, possess a specific and well-characterized prostaglandin synthase activity (*45*), it is tempting to speculate that the nonactivating conformer of Tyr10 may play a role in the prostaglandin D synthase activity of Sh28GST (M. Hervé, unpublished experiments). The proposed mechanism for PGDS involves two steps (*28*). In the first one, GSH adds to one oxygen atom in the peroxide ring of the prostaglandin, thereby breaking the O−O bond and forming a GSH addition intermediate; in the second step, an unidentified general base abstracts a proton from the carbon bonded to the first oxygen atom, consequently freeing the product PGD2 and leaving GSH bound to HPGDS. Upon comparison of the structures of Sh28GST and of HDGPS, it is clear that the Tyr10 side chain in the activating conformer would not allow enough space, being too close to the carbon atom of the substrate bound to the active site. However, if the Tyr10 side chain were to move to the nonactivating conformer after formation of an intermediate addition product, the space now available next to the carbon atom may be occupied by the unknown second general base, perhaps a water molecule activated by Arg16. In the case of Sh28GST, the PGDS activity may also be facilitated by the relatively high and unusual affinity of this enzyme for GSH, which would tend to ensure that the intermediate addition product remains bound to the protein. This hypothesis may also explain why a nonspecific PGDS activity is reported for GSTs.

A dual conformation of Tyr10 may possibly suggest a strategy for the development of inhibitors specific for the Sh28GST, and possibly other GSTs. The space occupied by Tyr10 in the activating conformer could be exploited in the design of inhibitors which would fill this cavity, essential to accommodation of the phenolic ring and duplication of the stabilizing polar contacts observed in the G-site containing this conformer. These (possibly stable) polar contacts for eliciting an inhibitor design include the H-bond with the main chain N atom of residue Arg14 and an H-bond or polar interaction with the guanidinium group of Arg16.

CONCLUSION

The crystal structure of Sh28GST, a member of the very well studied GST protein family, reveals new features concerning the role of the active site residues, the structure of the dimer interface, and the affinity for GSH. Two active site residues with previously well defined roles in structure

and function, Tyr10 and Arg16, were found to have additional, or perhaps previously unrecognized, stereochemical features. These two residues may have acquired a role in supporting different functions, such as the new functions that evolved for active site residues in the zeta and omega classes of GSTs (*54*−*57*). In general, it may be envisaged that Sh28GST is a multifunctional enzyme, which evolved to catalyze more than one reaction, as already suggested for other GSTs (*45*), and thus is not highly specialized. It may indeed be suggested that the major role played by Sh28GST in the schistosome is the synthesis of PGD_2, given the relevance of this pathway to the pathogenesis of the disease (*14*), and conversely that the GST activity is a remarkably well preserved evolutionary remnant, possibly of more limited physiological significance in the parasite.

The nonactivating second conformer of the highly conserved Tyr10 at the active site, which was not previously reported, is especially intriguing. From inspection of the crystal structure (Figures 3 and 6) and from crystallization experiments starting from free, partially saturated, or almost fully GSH saturated enzyme, the two conformers do not appear to change in relative population, certainly not in the crystal. Evidence from solution studies carried out on other GSTs, which demonstrated the high conformation flexibility, especially of the apoprotein, suggests that interconversion of the two Tyr10 conformers might be possible in solution; however, we do not know if this is the case for Sh28GST.

The several classes of GSTs can be distinguished by functional and structural properties (*6*), which are however difficult to predict from sequence analyses, given the low degree of similarity in the primary structure within the GST family. Now that the Sh28GST structure has been determined at high resolution (1.65−1.85 Å), two distinct structural features can be used to further classify the schistosome GSTs. The first is an elongation of the four-stranded β-sheet in the N-terminal domain (see Figure 2), which was not predicted by sequence alignment, and the second is a dimer interface which is rather polar (like PGDS and sigma class GSTs) and has a relatively limited interaction surface. The fact that the usual classification of GSTs is poorly suited to schistosomal enzymes should not come as a surprise given that it was originally devised for the mammalian proteins; thus, these different structural features, when combined with previous observations of a low degree of sequence similarity to other classes (∼30%), with the similarity of GSH interaction with that observed in mu class GSTs (*6*), and with the recent confirmation that Sh28GST is a specific PGDS, may suggest that schistosomal GSTs should be placed in a class of their own.

The most practical results emerging from analysis of the three-dimensional structure of Sh28GST may be the discovery of the relatively high affinity of the enzyme for GSH and the lack of inhibition of its transferase activity by praziquantel. We envisage that the protein used in vaccine trials is likely to have some GSH bound; consequently, there may be an unexpected effect of GSH on the antigenic properties of Sh28GST. With regard to praziquantel, the list of possible targets for this unique broad spectrum antischistosomal drug is now empty because neither Sj26GST (*27*) nor Sh28GST is inhibited. The novel features found in the active site of the crystal structure of Sh28GST, extensively discussed above, may help in discovery of specific inhibitors, which may or may not be effective against schistosomiasis, but would certainly be useful for studying directly the role of Sh28GST in infection.

ACKNOWLEDGMENT

We are grateful to ELETTRA (Trieste, Italy) and DESY (Hamburg, Germany) for the use of the synchrotron facility for X-ray crystallography.

REFERENCES

1. World Health Organization (1993) Expert Comitee on the Control of Schistosomiasis. The control of schistosomiasis, WHO Technical Report 830, World Health Organization, Geneva. World Health Organization (1996) Fact sheet on schistosomiasis, World Health Organization, Geneva.
2. Foster, J. M., and Johnston, D. A. (2002) Helminth genomics: from gene discovery to genome sequencing, *Trends Parasitol. 18*, 241−242.
3. Capron, A., Capron, M., Dombrowicz, D., and Riveau, G. (2001) Vaccine strategies against schistosomiasis: from concepts to clinical trials, *Int. Arch. Allergy Immunol. 124*, 9−15.
4. Balloul, J. M., Sondermeyer, P., Dreyer, D., Capron, M., Grzych, J. M., Pierce, R. J., Carvallo, D., Lecocq, J. P., and Capron, A. (1987) Molecular cloning of a protective antigen of schistosomes, *Nature 326*, 149−153.
5. Taylor, J. B., Vidal, A., Torpier, G., Meyer, D. J., Roitsch, C., Balloul, J. M., Southan, C., Sondermeyer, P., Pemble, S., and Lecocq, J. P., (1988) The glutathione transferase activity and tissue distribution of a cloned Mr28K protective antigen of *Schistosoma mansoni*, *EMBO J. 7*, 465−472.
6. Sheehan, D., Meade, G., Foley, V. M., and Dowd, C. A. (2001) Structure, function and evolution of glutathione transferases: implications for classification of non-mammalian members of an ancient enzyme superfamily, *Biochem. J. 360*, 1−16.
7. Balloul, J. M., Grzych, J. M., Pierce, R. J., and Capron, A. (1987) A purified 28,000 dalton protein from *Schistosoma mansoni* adult worms protects rats and mice against experimental schistosomiasis, *J. Immunol. 138*, 3448−3453.
8. Riveau, G., Poulain-Godefroy, A. P., Dupre, L., Remoue, F., Mielcarek, N., Locht, C., and Capron, A. (1998) Glutathine S-transferases of 28 kDa as major vaccine candidates against schistosomiasis, *Mem. Inst. Oswaldo Cruz 93* (Suppl. 1), 87−94.
9. Boulanger, D., Warter, A., Sellin, B., Lindner, V., Pierce, R. J., Chippaux, J.-P., and Capron, A. (1999) Vaccine potential of a recombinant glutathione S-transferase cloned from *Schistosoma haematobium* in primates experimentally infected with an homologous challenge, *Vaccine 17*, 319−326.
10. Scott, J. C., and McManus, D. P. (2000) Molecular cloning and enzymatic expression of the 28-kDa glutathione S-transferase of *Schistosoma japonicum*: evidence for sequence variation but lack of consistent vaccine efficacy in the murine host, *Parasitol. Int. 49*, 289−300.
11. Xu, C. B., Verwaerde, C., Grzych, J. M., Fontaine, J., and Capron, A. (1991) A monoclonal antibody blocking the *Schistosoma mansoni* 28-kDa glutathione S-transferase activity reduces female worm fecundity and egg viability, *Eur. J. Immunol. 21*, 1801−1807.
12. Grzych, J.-M., Grezel, D., Xu, C. B., Neyrinck, J.-L., Capron, M., Ouma, J. H., Butterworth, A. E., and Capron, A. (1993) IgA antibodies to a protective antigen in human schistosomiasis mansoni, *J. Immunol. 150*, 527−535.
13. Remoué, F., Mani, J.-C., Pugnière, M., Schact, A.-M., Capron, A., and Riveau, G. (2002) Functional specific binding of testosterone to *Schistosoma haematobium* 28-kilodalton glutathione S-transferase, *Infect. Immun. 70*, 601−605.
14. Angeli, V., Faveeuw, C., Roye, O., Fontaine, J., Teissier, E., Capron, A., Wolowczuk, I., Capron, M., and Trottein, F. (2001) Role of the parasite-derived prostaglandin D_2 in the inhibition of epidermal Langerhans cell migration during schistosomiasis infections, *J. Exp. Med. 193*, 1135−1147.
15. Trottein, F., Vaney, M.-C., Bachet, B., Pierce, R.-J., Colloc'h, N., Lecocq, J.-P., Capron, A., and Mornon, J.-P. (1992) Crystallization and preliminary X-ray diffraction studies of a protective cloned 28 kDa glutathione S-transferase from *Schistosoma mansoni*, *J. Mol. Biol. 224*, 515−518.

16. Lien, L., Gustafsson, A., Andersson, A.-K., and Mannervik, B. (2001) Human glutathione transferase A1-1 demonstrates both half-of-the-sites and all-of-the-sites reactivity, *J. Biol. Chem. 276*, 35599−35605.
17. Otwinowski, Z., and Minor, W. (1997) Processing of X-ray Diffraction Data Collected in Oscillation Mode, *Methods Enzymol. 276*, 307−326.
18. Navaza, J. (1994) AMoRe: an Automated Package for Molecular Replacement, *Acta Crystallogr. 50*, 157−163.
19. Collaborative Computational Project, Number 4 (1994) The CCP4 Suite: Programs for Protein Crystallography, *Acta Crystallogr. D50*, 760−763.
20. Murshudov, G. N., Vagin, A. A., and Dodson, E. J. (1997) Refinement of Macromolecular Structures by the Maximum-Likelihood Method, *Acta Crystallogr. D53*, 240−255.
21. McRee, D. E. (1999) XtalView/Xfit: A Versatile Program for Manipulating Atomic Coordinates and Electron Density, *J. Struct. Biol. 125*, 156−165.
22. Dietze, E. C., Wang, R. W., Lu, A. Y. H., and Atkins, W. M. (1996) Ligand effects on the fluorescence properties of tyrosine 9 in alpha 1-1 glutathione S-transferase, *Biochemistry 35*, 6745−6753.
23. Jakobson, I., Warholm, M., and Mannervik, B. (1979) The binding of substrates and a product of the enzymatic reaction to glutathione S transferase A, *J. Biol. Chem. 254*, 7085−7089.
24. Mannervick, B., and Guthenberg, C. (1981) Glutathione transferase (human placenta), *Methods Enzymol. 77*, 231−235.
25. Widersten, M., Kolm, R. H., Bjornsted, R., and Mannervick, B. (1992) Contribution of five amino acid residues in the glutathione binding site to the function of the human glutathione S-transferase P1-1, *Biochem. J. 285*, 377−381.
26. Laskowski, R. A., McArthur, M. W., Moss, D. S., and Thornton, J. M. (1993) PROCHECK: a program to check the stereochemical quality of protein structures, *J. Appl. Crystallogr. 26*, 283−291.
27. McTigue, M. A., DeWight, R. W., and Tainer, J. A. (1995) Crystal structure of a schistosomal drug and vaccine target: glutathione S-transferase from *Schistosoma japonicum* and its complex with the leading anti-schistosomal drug praziquantel, *J. Mol. Biol. 246*, 21−27.
28. Kanaoka, T., Ago, H., Inagaki, E., Nanayama, T., Miyano, M., Kikuno, R., Fujii, Y., Eguchi, N., Toh, H., Urade, Y., and Hayaishi, O. (1997) Cloning and crystal structure of hematopoietic prostaglandin D-synthase, *Cell 90*, 1085−1095.
29. Wilce, M. C., and Parker, M. W. (1994) Structure and function of glutathione S-transferases, *Biochim. Biophys. Acta 1205* (1), 1−18.
30. Armstrong, R. N. (1997) Structure, catalytic mechanism, and evolution of the glutathione transferases, *Chem. Res. Toxicol. 10*, 2−8.
31. Ji, X., von Rosenvinge, E. C., Johnson, W. W., Tomarev, S. I., Piatigorsky, J., Armstrong, R. N., and Gilliland, G. L. (1995) Three-dimensional structure, catalytic properties, and evolution of a sigma class glutathione transferase from squid, a progenitor of the lens S-crystallins of cephalopods, *Biochemistry 34*, 5317−5328.
32. Trottein, F., Godin, C., Pierce, R. J., Sellin, B., Taylor, M. G., Gorillot, I., Silva, M. S., Lecocq, J. P., and Capron, A. (1992) Inter-species variation of schistosome 28-kDa glutathione S-transferases, *Mol. Biochem. Parasitol. 54*, 63−72.
33. Koehler, R. T., Villar, H. O., Bauer, K. E., and Higgins, D. L. (1997) Ligand-based protein alignment and isozyme specificity of glutathione S-transferase inhibitors, *Proteins 28*, 202−216.
34. Gu, Y., Singh, S. V., and Ji, X. (2000) Residue R216 and catalytic efficiency of a murine class alpha glutathione S-transferase toward benzo[*a*]pyrene 7(R),8(S)-diol 9(S),10(R)-epoxide, *Biochemistry 39*, 12552−12557.
35. Oakley, A. J., Bello, M. L., Battistoni, A., Ricci, G., Rossjohn, J., Villar, H. O., and Parker, M. W. (1997) The structures of human glutathione transferase P1-1 in complex with glutathione and various inhibitors at high resolution, *J. Mol. Biol. 274*, 84−100.
36. Xiao, B., Singh, S. P., Nanduri, B., Awasthi, Y. C., Zimniak, P., and Ji, X. (1999) Crystal structure of a murine glutathione S-transferase in complex with a glutathione conjugate of 4-hydroxynon-2-enal in one subunit and glutathione in the other: evidence of signaling across the dimer interface, *Biochemistry 38*, 11887−11894.
37. Lim, K., Ho, J. X., Keeling, K., Gilliland, G. L., Ji, X., Ruker, F., and Carter, D. C. (1994) Three-dimensional structure of *Schistosoma japonicum* glutathione S-transferase fused with a six-amino acid conserved neutralizing epitope of gp41 from HIV, *Protein Sci. 3*, 2233−2244.
38. Ibarra, C., Nieslanik, B. S., and Atkins, W. M. (2001) Contribution of aromatic−aromatic interactions to the anomalous pK_a of tyrosine-9 and the C-terminal dynamics of glutathione S-transferase, *Biochemistry 40*, 10614−10624.
39. Liu, S., Ji, X., Gilliland, G. L., Stevens, W. J., and Armstrong, R. N. (1993) Second-sphere electrostatic effects in the active site of glutathione S-transferase. Observation of an on-face hydrogen bond between the side chain of threonine 13 and the Π-cloud of the tyrosine 6 and its influence on catalysis, *J. Am. Chem. Soc. 115*, 7910−7911.
40. Orozco, M., Vega, C., Parraga, A., Garcia-Saez, I., Coll, M., Walsh, S., Mantle, T. J., and Luque, F. J. (1997) On the reaction mechanism of class pi glutathione S-transferase, *Proteins: Struct., Funct., Genet. 28*, 530−542.
41. Christ-Hazelhof, E., Nugteren, D. H., and Van Dorp, D. A. (1976) Conversions of prostaglandin endoperoxides by glutathione-S transferases and serum albumins, *Biochim. Biophys. Acta 450*, 450−461.
42. Urade, Y., Fujimoto, N., Ujihara, M., and Hayaishi, O. (1987) Biochemical and immunological characterization of rat spleen prostaglandin D synthetase, *J. Biol. Chem. 262*, 3820−3825.
43. Pinzar, E., Miyano, M., Kanaoka, Y., Urade, Y., and Hayaishi, O. (2000) Structural basis of hematopoietic prostaglandin D synthase activity elucidated by site-directed mutagenesis, *J. Biol. Chem. 275*, 31239−31244.
44. Thomson, A. M., Meyer, D. J., and Hayes, J. D. (1998) Sequence, catalytic properties and expression of chicken glutathione-dependent prostaglandin D2 synthase, a novel class sigma glutathione S-transferase, *Biochem. J. 333*, 317−325.
45. Jowsey, I. R., Thomson, A. M., Flanagan, J. U., Murdock, P. R., Moore, G. B. T., Meyers, D. J., Murphy, G. J., Smith, S. A., and Hayes, H. D. (2001) Mammalian class sigma glutathione S-transferases: catalytic properties and tissue-specific expression of human and rat GSH-dependent prostaglandin D2 synthases, *Biochem. J. 349*, 507−516.
46. Milhon, J. L., Thiboldeaux, R. L., Glowac, K., and Tracy, J. W. (1997) *Schistosoma japonicum* GSH S-transferase Sj26 is not the molecular target of praziquantel action, *Exp. Parasitol. 87*, 268−274.
47. Ji, X., Von Rosenvinge, E. C., Johnson, W. W., Armstrong, R. N., and Gilliland, G. L. (1996) Location of a potential transport binding site in a sigma class glutathione transferase by X-ray crystallography, *Proc. Natl. Acad. Sci. U.S.A. 93*, 8208−8213.
48. Hubatsch, I., and Mannervik, B. (2001) A highly acidic tyrosine 9 and a normally titrating tyrosine 212 contribute to the catalytic mechanism of human glutathione transferase A4-4, *Biochem. Biophys. Res. Commun. 280*, 878−882.
49. Ricci, G., Caccuri, A. M., Bello, M. L., Rosato, N., Mei, G., Nicotra, M., Chiessi, E., Mazzetti, A. P., and Federici, G. (1996) Structural flexibility modulates the activity of human glutathione transferase P1-1. Role of helix flexibility in the catalytic mechanism, *J. Biol. Chem. 271*, 16187−16192.
50. Stella, L., Caccuri, A. M., Rosato, N., Nicotra, M., Lo Bello, M., De Matteis, F., Mazzetti, A. P., Federici, G., and Ricci, G. (1998) Flexibility of helix 2 in the human glutathione transferase P1-1. Time-resolved fluorescence spectroscopy, *J. Biol. Chem. 273*, 23267−23273.
51. Hitchens, T. K., Mannervik, B., and Rule, G. S. (2001) Disorder-to-order transition of the active site of human class pi glutathione transferase, GST P1-1, *Biochemistry 40*, 11660−11669.
52. Ricci, G., Del Boccio, G., Pennelli, A., Lo Bello, M., Petruzzelli, R., Caccuri, A. M., Barra, D., and Federici, G. (1991) Redox forms of human placenta glutathione transferase, *J. Biol. Chem. 266*, 21409−21415.
53. Lo Bello, M., Nuccetelli, M., Chiessi, E., Lahm, A., Mazzetti, A. P., Battistoni, A., Caccuri, A. M., Oakley, A. J., Parker, M. W., Tramontano, A., Federici, G., and Ricci, G. (1998) Mutations of Gly to Ala in human glutathione transferase P1-1 affect helix 2 (G-site) and induce positive cooperativity in the binding of glutathione, *J. Mol. Biol. 284*, 1717−1725.
54. Polekhina, G., Board, P. G., Blackburn, A. C., and Parker, M. W. (2001) Crystal structure of maleylacetoacetate isomerase/glutathione transferase zeta reveals the molecular basis for its remarkable catalytic promiscuity, *Biochemistry 40*, 1567−1576.
55. Thom, R., Dixon, D. P., Edwards, R., Cole, D. J., and Laphorn, A. J. (2001) The structure of a zeta class glutathione S-transferase from *Arabidopsis thaliana*: characterization of a GST with novel

active-site architechture and a putative role in tyrosine catabolism, *J. Mol. Biol. 308*, 949−962.
56. Todd, A. E., Orengo, C. A., and Thornton, J. M. (2002) Plasticity of enzyme active sites, *Trends Biochem. Sci. 27*, 419−425.
57. Board, P. G., Coggan, M., Chelvanayagam, G., Easteal, S., Jermiin, L. S., Schulte, G. K., Danley, D. E., Hoth, L. R., Griffor, M. C., Kamath, A. V., Rosner, M. H., Chrunyk, B. A., Perregaux, D. E., Gabel, C. A., Geoghegan, K. F., and Pandit, J. (2000) Identification, characterization, and crystal structure of the omega class glutathione transferases, *J. Biol. Chem. 275*, 24798−24806.

BI034449R